

UCLA

UCLA Previously Published Works

Title

Precipitation and vegetation shape patterns of genomic and craniometric variation in the central African rodent *Praomys misonnei*

Permalink

<https://escholarship.org/uc/item/6gg3n5vc>

Journal

Proceedings of the Royal Society B, 287(1930)

ISSN

0962-8452

Authors

Morgan, Katy
Mboumba, Jean-François
Ntie, Stephan
et al.

Publication Date

2020-07-08

DOI

10.1098/rspb.2020.0449

Peer reviewed



Research

Cite this article: Morgan K *et al.* 2020
Precipitation and vegetation shape patterns of
genomic and craniometric variation in the
central African rodent *Praomys misonnei*.
Proc. R. Soc. B **287**: 20200449.
<http://dx.doi.org/10.1098/rspb.2020.0449>

Received: 27 February 2020
Accepted: 12 June 2020

Subject Category:

Genetics and genomics

Subject Areas:

evolution, genetics, ecology

Keywords:

population genomics, climate change,
ecotones, generalized dissimilarity modelling,
gradient forest, landscape genomics

Author for correspondence:

Katy Morgan
e-mail: kmorganuno@gmail.com

Electronic supplementary material is available
online at <https://doi.org/10.6084/m9.figshare.c.5036327>.

Precipitation and vegetation shape patterns of genomic and craniometric variation in the central African rodent *Praomys misonnei*

Katy Morgan¹, Jean-François Mboumba², Stephan Ntie², Patrick Mickala², Courtney A. Miller¹, Ying Zhen³, Ryan J. Harrigan³, Vinh Le Underwood³, Kristen Ruegg³, Eric B. Fokam⁴, Geraud C. Tasse Taboue⁴, Paul R. Sesink Clee⁵, Trevon Fuller³, Thomas B. Smith³ and Nicola M. Anthony¹

¹Department of Biological Sciences, University of New Orleans, New Orleans, LA, USA

²Département de Biologie, Université des Sciences et Techniques de Masuku, Franceville, Gabon

³Centre for Tropical Research, Institute of Environment and Sustainability, University of California, Los Angeles, CA, USA

⁴Department of Zoology and Animal Physiology, University of Buea, Buea, Cameroon

⁵Department of Biology, Drexel University, Philadelphia, PA, USA

KM, 0000-0001-5326-4382; TF, 0000-0001-9954-4267

Predicting species' capacity to respond to climate change is an essential first step in developing effective conservation strategies. However, conservation prioritization schemes rarely take evolutionary potential into account. Ecotones provide important opportunities for diversifying selection and may thus constitute reservoirs of standing variation, increasing the capacity for future adaptation. Here, we map patterns of environmentally associated genomic and craniometric variation in the central African rodent *Praomys misonnei* to identify areas with the greatest turnover in genomic composition. We also project patterns of environmentally associated genomic variation under future climate change scenarios to determine where populations may be under the greatest pressure to adapt. While precipitation gradients influence both genomic and craniometric variation, vegetation structure is also an important determinant of craniometric variation. Areas of elevated environmentally associated genomic and craniometric variation overlap with zones of rapid ecological transition underlining their importance as reservoirs of evolutionary potential. We also find that populations in the Sanaga river basin, central Cameroon and coastal Gabon are likely to be under the greatest pressure from climate change. Lastly, we make specific conservation recommendations on how to protect zones of high evolutionary potential and identify areas where populations may be the most susceptible to climate change.

1. Introduction

Anthropogenic climate change is one of the greatest threats currently facing biodiversity [1]. The future survival of animal populations is likely to depend not only on their capacity to move to suitable habitats but also their ability to respond genetically or plastically to rapidly changing environments [2]. Standing genomic and phenotypic variation provides the raw material upon which natural selection can act (e.g. [3–5]), and as such may facilitate rapid evolutionary change [2]. In this regard, the development of methods for inferring gene–environment associations (GEAs) has provided opportunities to identify the environmental drivers underlying genomic differentiation [6] and to map areas of elevated genomic turnover, defined as the change in allelic composition with geographical distance. Such areas of elevated genomic turnover are likely to be important to conservation

because they may harbour populations that have the greatest capacity to adapt (e.g. [7,8]). In particular, populations distributed across strong ecological gradients may be important reservoirs of both phenotypic and genomic variation (e.g. [7,9,10]), since strong selection pressures imposed by environmentally heterogeneous landscapes are likely to have driven differentiation over time. Shifts in GEAs under climate change have also been used to identify areas with high genomic mismatch or 'offset', defined as the difference in allele frequencies predicted under future and current environmental conditions. These areas have been shown to be predictors of demographic decline and as such may constitute important regions where species are most vulnerable to climate change [11,12]. Therefore, mapping spatial patterns of environmentally associated variation under current and future climate conditions may not only help us to identify where species' adaptive capacity is likely to be the greatest but also pinpoint areas where adaptation to future climates is expected to require significant shifts in allele frequencies (e.g. [11,12]).

Tropical forests are one of the most important reservoirs of terrestrial biodiversity and have become increasingly vulnerable to climate change. Equatorial Africa in particular is likely to be severely impacted by future changes in temperature and precipitation [13]. This region harbours the second largest block of contiguous rainforest in the world [14] and is home to an estimated one-fifth of all known plant and animal species. Within this major rainforest block, the Lower Guinean phytogeographic region constitutes an important centre of plant endemism [15]. Environmental heterogeneity across the region is high and strong selection pressures are likely to operate along existing gradients structured by precipitation, elevation and habitat differences across the forest–savanna ecotone [9,16]. Although previous phylogeographic studies have focused primarily on the role of riverine barriers and Pleistocene refugia in shaping patterns of genetic differentiation, more recent studies on rainforest vertebrates [8,17–21] and trees [22] support the influence of environmental gradients. However, most molecular research to date has been limited to a handful of neutral molecular markers and has not included genome-wide surveys that might capture potential targets of environmentally mediated selection.

Advances in high throughput sequencing provide opportunities to characterize patterns of environmentally associated variation across the genome [23,24]. Two complementary approaches have been applied to modelling GEAs and mapping turnover in genomic composition at the landscape level: gradient forest (GF) [25] and generalized dissimilarity modelling (GDM) [26]. GF is based on the nonparametric, tree-based machine learning random forest (RF) approach. Nonlinear regressions are used to estimate turnover or change in allele frequencies as a function of changes in the values of environmental predictors [25,27]. Although GF can incorporate potentially complex interactions between predictor variables, it cannot directly incorporate geographical distances. Spatial effects may be incorporated via Moran eigenvectors (MEMs), however, their interpretation may be complicated by their potential to capture unmeasured environmental variation [27]. GF has also been used extensively to predict changes in GEAs under future climate change in order to identify areas of maximal genomic offset where populations are likely to have to adapt the most in response to future change (e.g. [11,12,28–30]). In contrast to GF, GDM uses nonlinear pairwise matrix regression to model genomic differentiation between site

pairs as a function of pairwise geographical and/or environmental distances [26,27]. An advantage of this approach is that it can directly incorporate resistance matrices that capture the effect of historical barriers to gene flow in order to assess their relative importance in driving patterns of genomic differentiation (e.g. [7,17]). Recent studies using both GF and GDM to model GEAs have argued that both methods are complementary as they differ in the way that they model these associations [27,28].

The central African rodent *Praomys misonnei* is widely distributed across the Lower Guinean region and inhabits a broad range of forest habitats, making it well-suited to landscape-level studies of genomic and phenotypic variation. Previous mitochondrial phylogeographic studies of this species have uncovered considerable historical structure that has been attributed to the impacts of past forest refugia and/or riverine barriers [31]. Analyses of morphological variation have also shown that craniometric variation (i.e. skull shape) is highly variable and differs between geographically distinct clades [32]. Skull shape is known to be under environmentally mediated selection in other vertebrate species (e.g. [4,33]), providing a strong precedent for examining the role of environmental variables in shaping patterns of differentiation in this trait.

Here, we characterize patterns of genomic and craniometric variation in central African populations of *P. misonnei* to address the following five questions. (1) Which are the most important environmental predictors of genomic differentiation? (2) Where are the areas of greatest turnover in genomic composition and genomic offset? (3) Can genomic differentiation be better predicted by historical barriers to gene flow or current environmental conditions? (4) Is craniometric variation shaped by the same environmental variables as those influencing genomic variation? (5) Which single nucleotide polymorphisms (SNPs) are associated with craniometric variation and what is their function?

The approaches used to address these questions are illustrated in electronic supplementary material, figure S1. We first used GF to model patterns of environmentally associated genomic variation in order to identify areas of elevated turnover and then projected these associations under different climate change scenarios to identify regions of greatest genomic offset. Next, we used GDM to examine the relative importance of historical landscape barriers versus contemporary environmental factors in driving patterns of genomic differentiation. Lastly, we used RF to identify environmental predictors of craniometric variation and latent factor mixed modelling (LFMM) [34] to identify SNPs associated with one or more principal components (PCs) describing skull shape.

2. Methods

(a) Environmental, genomic and morphological datasets

(i) Environmental data

A total of 26 environmental variables characterizing variation in precipitation, temperature, altitude and vegetation were downloaded from various online resources (electronic supplementary material, table S1). These include 19 bioclimatic variables, elevation and five variables relating to vegetation structure (all data sources detailed in electronic supplementary material, table

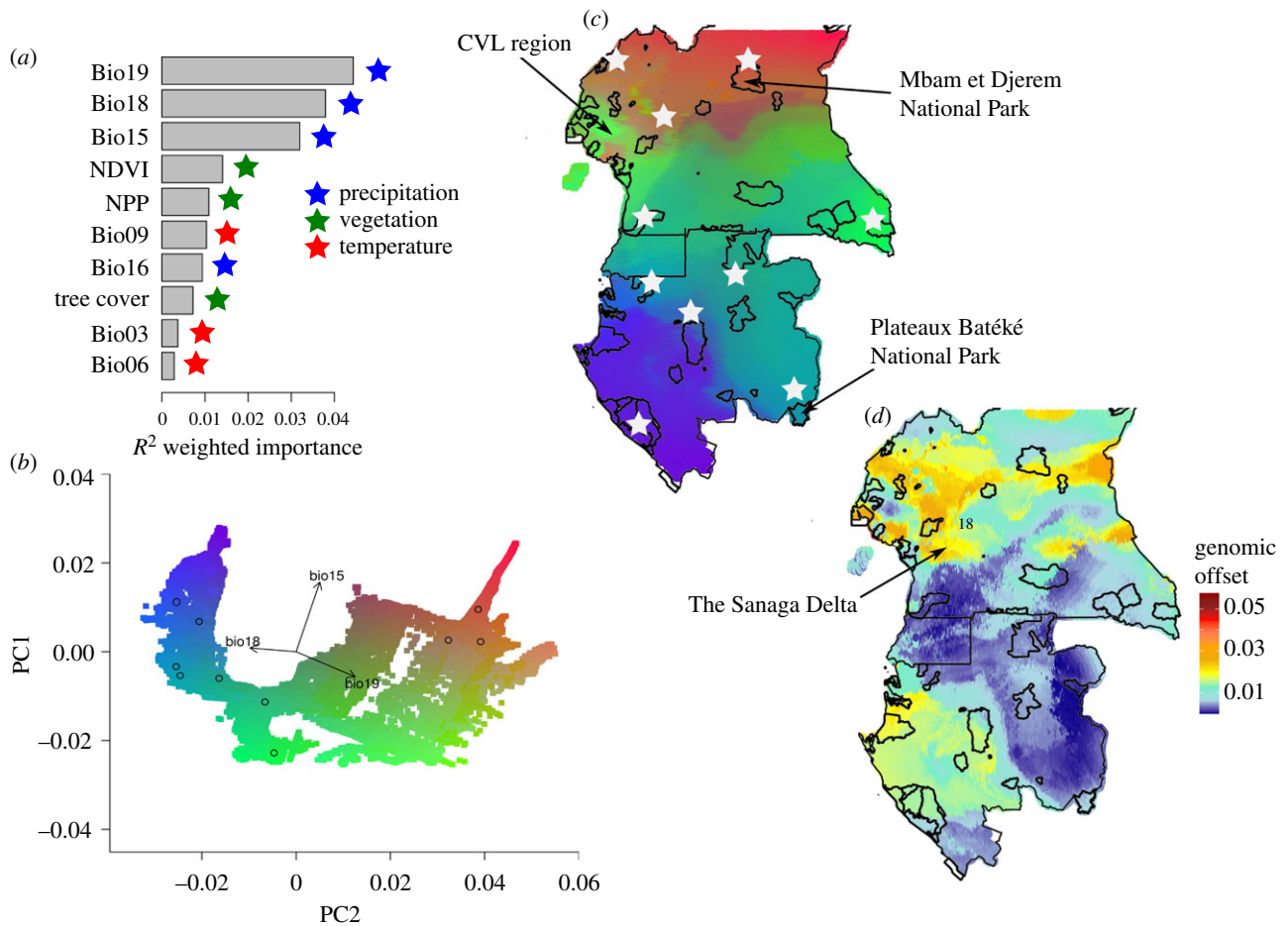


Figure 1. Influence of environmental variation on SNP allele frequencies, inferred through GF analysis. (a) Environmental variables ranked according to their importance in predicting allele frequency variation. Variables related to precipitation, temperature and vegetation are indicated by adjacent stars. (b) PCA plot illustrating the influence of environmental variation on predicted allele frequencies at 100 000 localities across central Africa. Pixel colour or shading represents predicted genotype and circled pixels indicate sampled localities. Arrow length and direction represent the strength and direction, respectively, of the influence of the three most important environmental predictors. (c) Predicted spatial turnover in allele frequencies projected over the study area. Black outlines indicate the location of current protected areas and white stars indicate sampling localities. (d) Spatial patterns of genomic offset, estimated using the 2080 RCP 8.5 climate projection. (Online version in colour.)

S1). To reduce collinearity in our dataset, we selected a subset of 10 reduced-correlation variables as described in the electronic supplementary material. All downstream analyses were performed with this subset of variables, which comprise several measures of temperature (bio03, bio06, bio09), precipitation (bio15, bio16, bio18, bio19) and vegetation structure (tree cover, net primary productivity (NPP), normalized difference vegetation index (NDVI) and potential evapotranspiration (PET)).

(ii) Genomic data

Adult *P. misonnei* were sampled from 10 localities across Gabon and Cameroon (figure 1c; electronic supplementary material, figure S2A) using baited live traps [35]. Genomic DNA was extracted using DNeasy kits (Qiagen, CA). Library preparation for restriction site-associated DNA sequencing (RAD-seq) was carried out following the protocol detailed in [36] and in the electronic supplementary material, methods. Processing of RAD-seq data was carried out using either (a) the Stacks v. 1.48 pipeline [37] followed by several additional steps outlined in [8], or (b) the maximum exact matches algorithm implemented in Burrows–Wheeler Aligner (BWA) to align RAD loci [38] before filtering and SNP calling in SAMtools [39]. Since both workflows gave similar results (see Results and electronic supplementary material, figure S3), we present data from the SNP dataset generated using the Stacks pipeline. Following quality control and filtering, we retained a single SNP randomly selected from

each RAD locus to generate a final dataset of 36 567 SNPs. Further details regarding the Stacks parameter optimization, quality control and filtering of RAD data can be found in the electronic supplementary material, methods.

(iii) Morphological data

The skull of each individual was extracted in the field and preserved in 70% ethanol. Measures of skull shape were generated using landmark morphometric analyses. Each skull was photographed and digitized using ImageJ [40], as described in the electronic supplementary material, methods. Homologous landmarks were chosen to cover all functional areas of the skull, including 20 landmarks on the dorsal surface and 16 landmarks on the ventral surface (figure 2). The effects of size, position and orientation were removed [40], and covariance matrices describing shape variation were generated from the resulting Procrustes shape coordinates.

Two sets of statistics were generated to describe shape variation in the dataset. First, matrices describing between-site shape distances were constructed in MorphoJ using Procrustes distance, which provides a measure of the absolute pairwise distance between group means, and Mahalanobis distance, which takes within-group variation into account [41]. Second, principal components analysis (PCA) was used to summarize inter-individual shape variation. PCA provides a method of reducing high dimensionality shape information into a smaller number of non-correlated axes [42] and was performed separately for each of the

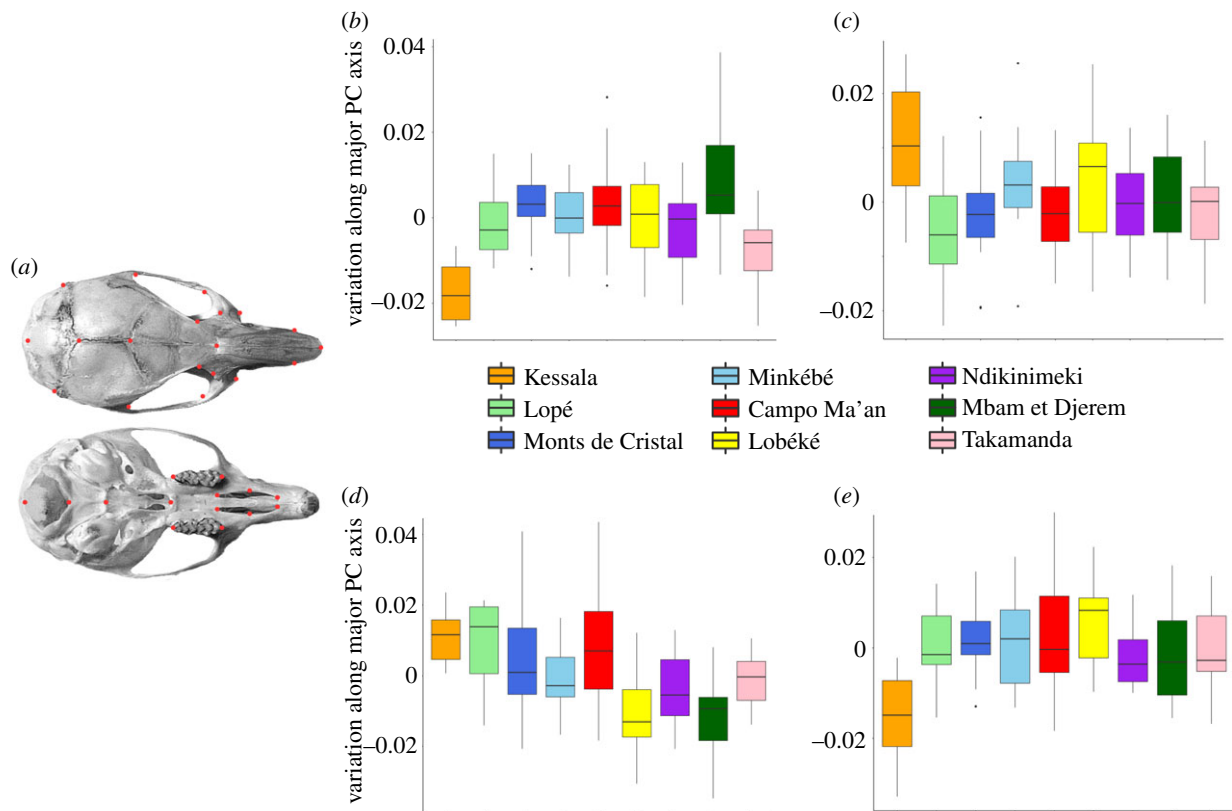


Figure 2. Variation in skull shape within sampled populations. (a) The placement of morphometric landmarks on the dorsal and ventral skull surfaces. (b–c) Variation in dorsal skull shape within sampled populations along the first and second PC axes, respectively. (d–e) Variation in ventral skull shape along the first and second PC axes, respectively. (Online version in colour.)

covariance matrices describing dorsal and ventral shape variation in MorphoJ. The top three dorsal and ventral PC axes were retained for downstream statistical analyses.

(b) Statistical analyses

(i) Gradient forest analyses of environmentally associated genomic turnover and future projections of genomic offset

The GF method implements a machine learning approach originally developed for the RF algorithm that combines individual decision trees to identify potentially complex relationships between predictor and response variables. According to the RF algorithm, each decision tree is grown from a random sample of the response data with replacement (bootstrap aggregation or ‘bagging’). At each node in the tree, a random subset of the predictor variables (features) is taken and used to partition the response data in a way that maximizes homogeneity within partitions. This process is repeated until the root-mean-squared error (MSE) of the model can no longer be reduced by further partitioning of the response variable. The bagging and feature randomness steps reduce correlations between trees, which are then combined into a single ensemble, or forest.

In GF, allele frequency data are treated as the biological response variable and partitioned at numerous split values along each environmental gradient. The amount of variation in SNP allele frequencies explained by each split value is termed the ‘split importance’. Moving along each environmental gradient, GF cumulatively sums split importance to create a step-like allele frequency turnover function, the maximum height of which reflects the overall importance of a given predictor in explaining allele frequency variation. According to the methodology developed by Ellis *et al.* [25] and further described in [27], SNPs with positive R^2 values are retained to construct an aggregate allele frequency turnover function, in which SNPs

are weighted according to their R^2 value and environmental predictors are weighted according to their relative importance. All GF modelling was carried out using the gradientForest R package. The analysis was run using 2000 regression trees for each of the 10 environmental predictor variables.

To assess whether our GF model performed better than random, the environmental-predictor matrix was shuffled to generate 200 randomized datasets and the performance of this random model was compared to that built on the real dataset. GF analyses were carried out both including ($n = 10$) and excluding ($n = 9$) the Gamba population, to ensure the small number of individuals sampled from this site (electronic supplementary material, figure S2A) did not affect model performance.

Using the three most important environmental predictors in the model, a continuous GEA surface describing environmentally associated allele frequency turnover was extrapolated across the study region using current climate conditions drawn from a set of 100 000 random points distributed across this area. This GEA surface was then projected under future climate, according to the four Intergovernmental Panel on Climate Change representative concentration pathways (RCPs) for 2080 [43]. The RCP predictions used in this study represent an aggregate of 20 global climate models (GCMs) [43] (see electronic supplementary material). To identify areas where GEAs are predicted to shift the most over the next 60 years, the model predicting allele frequencies under current conditions was subtracted from those predicted under the 2080 climate projection [44] in order to visualize areas where genomic offset is greatest.

(ii) Using generalized dissimilarity modelling to assess the importance of historical barriers versus contemporary environmental drivers

GDM uses permutational regression of site-by-site dissimilarity matrices to model pairwise differences in a biological response

variable as a function of pairwise dissimilarities in a range of predictor variables [26]. To accommodate nonlinear relationships between predictor and response variables, GDM fits a generalized linear model using I-spline transformed predictor variables. These I-spline turnover functions describe the rate of turnover in biological variation along each of a range of predictor variables. The height of each spline represents the total amount of biological variation explained by a given predictor, holding all other predictor variables constant.

The biological response matrix was based on either (1) Bray–Curtis dissimilarity between pairs of sites, based on the presence/absence of individual SNPs, or (2) pairwise F_{ST} values (see electronic supplementary material). Response matrices were created using SNPs that were either ‘environmentally associated’ or ‘background’. The former subset contained all SNPs included in the GF model (i.e. SNPs with positive R^2 values; see above) whereas the latter subset was made up of all remaining SNPs. Analyses were performed with and without the Gamba population.

Biological response matrices were regressed against a total of 13 predictor variable matrices describing pairwise environmental, geographical and resistance distances (designed to capture landscape features that may have historically represented barriers to gene flow). Environmental distances were based on pairwise site-site differences in the values of each of the 10 environmental variables described in section 2(a(i)) and electronic supplementary material, table S1. The geographical distance matrix was based on straight-line distances between sites. Two pairwise resistance matrices accounting for the presence of riverine barriers and shifts in habitat suitability during the last glacial maximum (LGM) of the Pleistocene were modelled using Circuitscape [45]. Past habitat suitability was predicted by constructing hindcast species distribution models (SDMs), using the maximum entropy modelling approach implemented in Maxent 3.4.1 [46] (see electronic supplementary material, methods). Given that the large number of predictor variables relative to the number of data points ($n = 45$) could lead to model over-fitting, we repeated our GDM analyses using only the three most important environmental variables identified by the GF analysis, alongside the geographical and two resistance distances, reducing the number of predictors to six. For all GDM runs, I-spline turnover functions describing the relationship between the biological response variable and each of the predictor matrices were visualized using rug plots and their significance was tested using 1000 permutations.

(iii) Multivariate analyses of craniometric variation

The significance of pairwise shape distances between sampling localities was assessed using permutation tests, which involve repeatedly randomizing the dataset and recalculating Procrustes and Mahalanobis distances to determine whether observed distances between populations are significantly greater than those calculated using randomized data. A total of 10 000 permutations were performed. The Gamba population was excluded from this analysis due to the low sample size (electronic supplementary material, figure S2A).

The influence of sex and sampling locality on inter-individual shape variation along the three major dorsal and ventral PC axes was examined using ANOVA using the `avov()` R function [47]. The influence of each of the 10 environmental variables on inter-individual shape variation along the major PC axes was tested using RF regression models, performed using individuals from all sampled populations and the `randomforest` R package [48]. Details on run parameters can be found in the electronic supplementary material, methods.

(iv) Associations between individual SNPs and craniometric data

To determine whether craniometric variation is associated with variation at any of the 36 567 SNP loci, LFMM [34] was

used to identify relationships between allele frequencies at each individual SNP with variation along each of the major PC axes describing dorsal and ventral skull shape variation. RAD loci containing SNPs that showed a significant association with skull shape were further interrogated by surveying the most closely related rodent genome (*Mus musculus*) for homologous loci using the basic local alignment tool (BLAST) algorithm.

3. Results

(a) Generation of genomic and morphological datasets

(i) Genomic data

Genomic data were generated for a total of 132 adult *P. misonnei*, sampled from 10 populations distributed across Gabon and Cameroon (see electronic supplementary material, figure S2A; figure 1c). Results from PCA, fastSTRUCTURE [49] and GF (see below) analyses were highly consistent for SNP datasets generated either via STACKS or the BWA and SAMtools pipeline and reveal high population structure in our dataset (electronic supplementary material, figures S2 and S3). Our final, filtered SNP set comprised a total of 36 567 SNPs. Although there was relatively low mean coverage range across individuals (7.2–12.2 \times), the consistency obtained across datasets indicates our findings are robust to the potentially confounding effects of erroneously called alleles.

(ii) Craniometric data

Data describing skull shape variation were generated from 169 individuals sampled from the 10 populations shown in electronic supplementary material, figure S2A and figure S1C. Centroid size (CS) explains 26.33% of variation in dorsal skull shape and 25.86% of variation in ventral skull shape. Once the effect of size was removed, plots of major PC axes indicated substantial overlap in skull shape between males and females (electronic supplementary material, figure S4), thus data from both sexes was combined for further analysis. The top three PCs explain 26.89, 14.08 and 12.20% of total dorsal shape variation, and 29.36, 16.08 and 13.85% of total ventral shape variation.

(b) Statistical analyses

(i) Gradient forest modelling of genomic turnover and genomic offset under future climate scenarios

In the GF model, 5649 out of 36 567 (15.45%) SNPs showed R^2 values > 0 (range: 0.00021–0.64, mean: 0.17). Both the number of SNPs with positive R^2 values and the mean R^2 value generated for the real dataset fell above the upper 95% quartile of values from the randomized datasets (see electronic supplementary material, figure S5), indicating the GF model performed better than random. Of the environmental predictor variables included in the GF model, the three with the strongest influence were the precipitation variables Bio15, Bio18 and Bio19 (figure 1a). We obtained very similar results when the Gamba population was excluded from the model, indicating that low sample size did not influence our findings.

Using these top three environmental predictors, GF was used to generate a continuous surface of environmentally associated genomic turnover across the study region. This projection provided strong support for high genomic turnover in several areas, notably: the forest–savanna transition zone spanning central Cameroon, the Cameroon Volcanic

Line (CVL) in southwest Cameroon, the region spanning the equator separating Cameroon from Gabon and the coast to interior precipitation gradient in Gabon (figure 1*b,c*). Subtracting predicted allele frequencies under current conditions from those predicted under future climate change (2080) revealed several zones of high genomic offset in Cameroon and to a lesser extent in coastal Gabon (figure 1*d*; electronic supplementary material, figure S6).

(ii) Generalized dissimilarity modelling analyses of historical barriers versus contemporary drivers of genomic differentiation

In GDM analyses fitted with the full set of 13 explanatory variables, three environmental variables (Bio18, Bio19 and NPP) and geographical distance were consistently significant predictors of genomic differentiation. This finding was true for both the 'environmentally associated' and 'background' SNP datasets and for both biological response matrices constructed from either pairwise Bray–Curtis dissimilarity matrices (environmentally associated SNPs—Bio18: $p = 0.046$, NPP: $p = 0.018$, geographical distance: $p < 0.001$; background SNPs—Bio18: $p = 0.017$, NPP: $p = 0.026$, geographical distance: $p = 0.001$) or pairwise F_{ST} statistics (environmentally associated SNPs—Bio18: $p = 0.01$, geographical distance: $p < 0.001$; background SNPs—Bio19: $p = 0.02$, geographical distance: $p = 0.001$). Neither of the two resistance matrices modelling the effects of riverine barriers or the distribution of suitable habitat since the LGM had any significant effect on the model.

When GDM models were fitted using the top three environmental predictors from the GF model, geographical distance and the two resistance matrices, only geographical distance and the precipitation variable Bio19 were found to significantly influence genomic variation. This finding was true for both the 'environmentally associated' and 'background' SNP datasets and for both for biological response matrices constructed from pairwise Bray–Curtis dissimilarity matrices (environmentally associated SNPs—Bio19: $p = 0.021$, geographical distance: $p < 0.01$; background SNPs—Bio19: $p = 0.029$, geographical distance: $p = 0.01$) and pairwise F_{ST} statistics (environmentally associated SNPs—Bio19: $p = 0.029$, geographical distance: $p < 0.01$; background SNPs—Bio19: $p = 0.017$, geographical distance: $p < 0.01$). Once again, neither of the two resistance matrices had any significant effect on pairwise genomic differentiation. Taken together, these results indicate that precipitation variables Bio18 and/or Bio19 act in concert with geographical distance to shape patterns of genomic differentiation across the region.

(iii) Multivariate analyses of craniometric variation

Pairwise Procrustes and Mahalanobis distances were significantly differentiated between most populations, with those from Kessala in southeastern Gabon and Mbam et Djerem national park in central Cameroon showing particularly strong differentiation from all other sampled populations (electronic supplementary material, table S2). ANOVAs revealed a significant influence of population on variation along the top three PCs describing inter-individual dorsal craniometric variation (PC1: F -value = 7.375, $p < 0.001$; PC2: F -value = 2.996, $p < 0.01$; PC3: F -value = 4.936, $p < 0.001$) and the top two PCs describing ventral craniometric variation (PC1: F -value = 8.346, $p < 0.001$; PC2: F -value = 4.202, $p < 0.001$). The influence of population on variation along ventral

PC3 was not significant (F -value = 1.874, $p = 0.068$). Dorsal PCs 1, 2 and 3 describe variation in the shape of the zygomatic arch and skull vault, the shape of the nasal bone, and the depth of the skull vault, respectively (electronic supplementary material, figure S7). Populations from Kessala and Mbam et Djerem were distinct from one another and all other sampled populations along dorsal PC1, while dorsal PC2 differentiated Kessala from all other populations (figure 2*b,c*). Ventral PCs 1, 2 and 3 describe variation in the size and shape of the incisive foramen (electronic supplementary material, figure S7). Ventral PC1 mainly differentiates the southern Gabon populations adjacent to Lopé national park and Kessala from populations in the north and east of Cameroon, while PC2 mainly differentiates Kessala from all other populations (figure 2*d,e*).

The total amount of variation in dorsal PC1 explained by the environmental predictors in the RF model is 24.85%. NPP is the most important predictor of dorsal PC1 (MSE 63.17%), where MSE indicates the importance of each predictor variable. The precipitation variables Bio19 and Bio15 were the second and third most important predictors in the model (MSE 48.95% and 47.65%, respectively). With respect to ventral PC1, environmental variables were found to explain 21.67% of the total variation. Bio18 was identified as the most important predictor (MSE 64.72%), followed by NDVI and tree cover (MSE 46.08% and 44.6%, respectively). The RF model, however, showed low power for predicting variation along both dorsal and ventral PCs 2 and 3 using environmental predictors, hence we limit our interpretation to the first PC for both dorsal and ventral skull shape.

(iv) Associations between individual SNPs and craniometric data

LFMM analyses revealed a significant association between SNP variation and dorsal PC1, PC2 and PC3 axes (4, 9 and 31 SNPs, respectively) and ventral PC1, PC2 and PC3 axes (4, 34 and 70 SNPs, respectively). However, there was no overlap in loci detected on each axis. BLAST identified 38 RAD loci that were significantly associated with skull shape that fall within coding and annotated genomic regions of the *M. musculus* genome. These candidate genes have functions related to nervous system functioning, insulin secretion, response to nutrient levels, sensory perception of pain and regulation of transcription (electronic supplementary material, table S3).

4. Discussion

(i) Which are the most important environmental predictors of genomic variation?

Both GF and GDM models indicate that precipitation has a strong influence on patterns of genomic differentiation in *P. misonnei*. Lower Guinean rainforests experience highly variable patterns of rainfall, such that the timing, duration, frequency and magnitude of rainy seasons can change over short geographical distances [50]. Spatial and temporal variation in rainfall can be expected to have a profound influence on resource availability and habitat structure, both of which may exert strong selection pressures on local populations. Fine-scale analyses of genomic variation along regional precipitation gradients may provide novel insights

into the role of natural selection in driving the observed patterns of variation.

(ii) Where are the areas of greatest turnover in genomic composition and genomic offset?

The GF model predicted high environmentally associated genomic turnover across the savanna-forest gradient in Cameroon and along the CVL in southwestern corner of the country. Both regions have previously been identified as areas of high turnover in songbird populations, indicating their importance as drivers of diversification in the Lower Guinean region [8,16,21] as a result of strong diversifying selection [8,21]. Similarly, the high species richness and endemism in several taxonomic groups along the CVL has been attributed in part to the refugial history and strong elevational gradients of this region [51,52]. Our study also indicated a subtle break across the equator that may coincide with the seasonal inversion in rainfall patterns. Previous studies have suggested that this inversion may have played an important role in driving population structure in some rainforest trees [22]. While reproductive activity in central African rodents is generally thought to be year-round, peaks of elevated breeding have been reported during rainy seasons [53], potentially creating a partial barrier to reproduction. Further work in *P. misonnei* and other central African rodents is needed to test this hypothesis.

Regions of high genomic offset were predicted in several areas of Cameroon, notably: the Sanaga river delta, the CVL, and in the central Cameroon forest-savanna ecotone. While the neighbouring country of Gabon shows less pattern, much of the coast appears to be moderately vulnerable, presumably because this area generally receives greater rainfall and is thus more sensitive to shifts in precipitation. Previous studies in North American bird species have shown that predicted genomic offset is associated with recent population declines, suggesting that this metric can be used to identify areas where populations are struggling to adapt [11,12]. Although corresponding demographic data is not available for the present study, we can nevertheless speculate that areas of greatest genomic offset may suffer disproportionately from changes in climate.

(iii) Can genomic differentiation be better predicted by historical barriers to gene flow or current environmental conditions?

Overall, our results show that contemporary environmental variation plays an important role in shaping patterns of genomic variation in *P. misonnei* populations. Consistent with a previous mitochondrial phylogeographic study [31], we find support for strong population structure. However, our GDM analysis indicates that this structure is driven primarily by contemporary environmental variation and geographical distance rather than an effect of isolation due to riverine barriers or shifts in suitable habitat during the LGM, as has been hypothesized in previous studies of this species [31].

GDM identified a significant influence of environmental variation on genomic differentiation, both in the 'environmentally associated' SNPs that were included in the GF model and the remaining 'background' SNPs. This lack of effect of the choice of SNPs included in each model may be due to inherent

differences between the way that GF and GDM treat GEAs. Whereas GDM models pairwise genomic distances using a single statistic to summarize genomic differentiation, GF models changes in allele frequency for each SNP independently and then aggregates these responses to create a turnover function. Nevertheless, both models have merit in this analysis: GDM is distance-based and can accommodate geographical and resistance distances whereas GF can incorporate potentially complex interactions between environmental predictors [25,27]. Importantly, our GDM results show that precipitation gradients shape genome-wide pairwise differentiation between sites, independent of other explanatory variables, and that both GDM and GF recover the same environmental predictors of genomic differentiation.

(iv) Is craniometric variation shaped by the same environmental variables as those influencing genomic variation?

Since the phenotype is the target of natural selection, maintaining the processes that generate this diversity is likely to be important for preserving species' adaptive evolutionary potential. Small mammals are good models for exploring environmental drivers of phenotypic variation since skull morphology has been linked to one or more environmental variables (e.g. [34,54,55]). For example, temperature and precipitation were found to influence skull shape in two species of mice in the Sigmodontinae subfamily [56]. In a Brazilian spiny rat species, skull shape varied along a latitudinal and environmental gradient characterised by changes in temperature, rainfall and altitude [54]. Lastly, in another study of red-backed moles (*Myodes gapperi*), the shape of the zygomatic arch varied between populations sampled from regions that differ in temperature and precipitation [55]. It has been suggested that such variation is associated with differences in facial musculature, which may allow for improved processing of specific food types (reviewed in [55]). Hence differences in food resources may lead to increased selection pressures on craniometric variation (e.g. [57]).

We detected significant pairwise differences in skull shape between populations. The precipitation variable Bio18 was an important predictor of both genomic and ventral craniometric variation, suggesting that both are shaped by the same precipitation gradients. However, variables relating to vegetation structure were also found to be important in shaping craniometric variation along both dorsal and ventral axes. Moreover, populations at Mbam et Djerem in north-central Cameroon, Kessala in southeast Gabon and Lopé in central Gabon have distinct skull morphologies. All three sites lie in or close to forest-savanna ecotones and as such exhibit high heterogeneity in forest cover and structure, lower precipitation levels and greater variation in temperature and humidity [58]. This heterogeneity may lead to differences in food availability [59] that could ultimately drive craniometric differentiation.

(v) Which SNPs associate with skull shape and what is their function?

While phenotypic variation may have a plastic component, correlations between craniometric variation and individual SNPs might support an underlying genetic mechanism.

Several SNP loci were found to be associated with skull shape variation. Some of these loci map to annotated, coding regions of the *M. musculus* genome. Three of these genes, *Fam3b*, *Cps1* and *Abo*, are involved in insulin secretion and/or metabolic processes [60,61]. Several genes, including *Dlg2* and *Cpne6*, play roles in nervous system function and sensory perception [62,63], traits that may be under diversifying selection due to differences in predation pressure. Further work should focus on characterizing the influence of selection in shaping craniometric variation across the forest–savanna ecotone and the role that these candidate genes might play in adaptive diversification across this boundary.

(vi) Conservation implications

There are two schools of thought in prioritizing areas for conservation (reviewed in [64]). Proactive schemes focus on conserving sites in which threats to biodiversity are low, thus maximizing the likely success of conservation efforts. Reactive schemes focus on conserving sites under a high degree of threat where biodiversity is unlikely to survive without urgent intervention [64].

A proactive scheme would, therefore, prioritize areas with high genomic turnover and low genomic offset. Within the context of our study, the national park systems of both Cameroon and Gabon encompass a wide range of environmentally associated genomic variation, indicated by the different colours portrayed in figure 1c. Within Cameroon, Mbam et Djerem is of special note, since in addition to harbouring high levels of genomic turnover associated with the forest–savanna transition zone, it also contains individuals with unique craniometric variation. Within Gabon, individuals sampled from the ecotone region surrounding the Batéké Plateaux National Park in southeast Gabon also have a unique skull phenotype. This region has been shown to be an area of high genomic turnover in blue duikers [17] and encompasses unusually high levels of plant and amphibian diversity [65,66], suggesting that it too may warrant special conservation attention. However, while areas of unique genomic and/or phenotypic diversity are thus well-preserved by the national park systems, areas that capture

elevated turnover are not well represented and could be protected through corridors designed to span these gradients and connect existing reserves together.

By contrast, a reactive scheme would focus on areas of high genomic offset, regardless of levels of environmentally associated turnover. Areas of high genomic offset were found in the Sanaga river basin, along the CVL and across the savanna–forest transition in Cameroon (figure 1d). In Gabon, genomic offset was generally low except along coastal areas to the south, highlighting the potential vulnerability of this region to future climate change. Since high genomic offset has been found to predict demographic declines in wild populations [11,12], future work should focus on areas of elevated offset to determine how ongoing climate change may already be impacting population viability in these regions.

Ethics. All animal handling procedures were carried out according to an approved University of New Orleans Institutional Animal Care and Use Committee (IACUC) protocol number 12-009.

Data accessibility. The genomic and craniometric data generated in this study are available from the Dryad Digital Repository: <https://doi.org/10.5061/dryad.0k6djh9x8> [67].

Authors' contributions. K.M., J.-F.M., S.N., P.M., C.A.M., E.B.F., G.C.T.T. and N.M.A. were responsible for data collection. K.M., R.J.H., V.L.U. and K.R. performed the laboratory processing of samples. Data analysis was conceived and performed by K.M., C.A.M., Y.Z., R.J.H., P.R.S.C., T.B.S. and N.M.A. All authors contributed to the writing of the manuscript.

Competing interests. We declare we have no competing interests.

Funding. This work was supported by National Science Foundation grant no. OISE 1243524.

Acknowledgements. We thank the Agence Nationale des Parcs Nationaux (ANPN, Gabon), the Centre National de la Recherche Scientifique et Technologique (CENAREST, Gabon), the Ministère des Forêts et de la Faune (MINFOF, Cameroon) and the Ministère de la Recherche Scientifique et de l'innovation (MINRESI, Cameroon) for sampling permits (permit IDs: #AE130012, #AR0010/13, AR0024/14, #153/AO/MINFOF/PNCM and #008/A/MINFOF/R). We are grateful to Joanna G. Larson for her advice and valuable assistance in setting up sampling protocols, and to Michael Bruford, for providing feedback on the manuscript. We also thank our field guides, without whom sampling collection would not have been possible. Thanks to University of California, Berkeley's Vincent J. Coates Genomic Sequencing Laboratory (GSL), for providing sequencing services.

References

- Bellard C, Bertelsmeier C, Leadley P, Thuiller W, Courchamp F. 2012 Impacts of climate change on the future of biodiversity. *Ecol. Lett.* **15**, 365–377. (doi:10.1111/j.1461-0248.2011.01736.x)
- Sgrò CM, Lowe AJ, Hoffmann AA. 2011 Building evolutionary resilience for conserving biodiversity under climate change. *Evol. Appl.* **4**, 326–337. (doi:10.1111/j.1752-4571.2010.00157.x)
- Lai YT *et al.* 2019 Standing genetic variation as the predominant source for adaptation of a songbird. *Proc. Natl Acad. Sci. USA* **116**, 2152–2157.
- Lawson LP, Petren K. 2017 The adaptive genomic landscape of beak morphology in Darwin's finches. *Mol. Ecol.* **26**, 4978–4989. (doi:10.1111/mec.14166)
- Bitter MC, Kapsenberg L, Gattuso JP, Pfister CA. 2019 Standing genetic variation fuels rapid adaptation to ocean acidification. *Nat. Commun.* **10**, 1–10. (doi:10.1038/s41467-019-13767-1)
- Reilstab C, Gugerli F, Eckert AJ, Hancock AM, Holderegger R. 2015 A practical guide to environmental association analysis in landscape genomics. *Mol. Ecol.* **24**, 4348–4370. (doi:10.1111/mec.13322)
- Thomassen HA *et al.* 2010 Modeling environmentally associated morphological and genetic variation in a rainforest bird, and its application to conservation prioritization. *Evol. Appl.* **3**, 1–16. (doi:10.1111/j.1752-4571.2009.00093.x)
- Zhen Y, Harrigan RJ, Ruegg KC, Anderson EC, Ng TC, Lao S, Lohmueller KE, Smith TB. 2017 Genomic divergence across ecological gradients in the Central African rainforest songbird (*Andropadus virens*). *Mol. Ecol.* **26**, 4966–4977. (doi:10.1111/mec.14270)
- Schneider CJ, Smith TB, Larison B, Moritz C. 1999 A test of alternative models of diversification in tropical rainforests, ecological gradients vs. rainforest refugia. *Proc. Natl Acad. Sci. USA* **96**, 13 869–13 873. (doi:10.1073/pnas.96.24.13869)
- Oyamaguchi HM, Oliveira E, Smith TB. 2017 Environmental drivers of body size variation in the lesser treefrog (*Dendropsophus minutus*) across the Amazon-Cerrado gradient. *Biol. J. Linn. Soc.* **120**, 363–370. (doi:10.1111/bj.12879)
- Bay RA, Harrigan RJ, Le Underwood V, Gibbs HL, Smith TB, Ruegg K. 2018 Genomic signals of selection predict climate-driven population declines in a migratory bird. *Science* **359**, 83–86. (doi:10.1126/science.aan4380)

12. Ruegg K, Bay RA, Anderson EC, Saracco JF, Harrigan RJ, Whitfield M, Paxton EH, Smith TB. 2018 Ecological genomics predicts climate vulnerability in an endangered southwestern songbird. *Ecol. Lett.* **21**, 1085–1096. (doi:10.1111/ele.12977)
13. James R, Washington R. 2013 Changes in African temperature and precipitation associated with degrees of global warming. *Clim. Change* **117**, 859–872. (doi:10.1007/s10584-012-0581-7)
14. Mayaux P *et al.* 2006 Cartographie et évolution du couvert forestier en Afrique centrale. See <http://hdl.handle.net/2078.1/73586>.
15. White F. 1979 The Guineo-Congolian region and its relationships to other Phytochoria. *Bull. Jard. Bot. Belg.* **49**, 11–55. (doi:10.2307/3667815)
16. Smith TB. 1997 A role for ecotones in generating rainforest biodiversity. *Science* **276**, 1855–1857. (doi:10.1126/science.276.5320.1855)
17. Ntie S *et al.* 2017 Evaluating the role of Pleistocene refugia, rivers and environmental variation in the diversification of central African duikers (genera *Cephalophus* and *Philantomba*). *BMC Evol. Biol.* **17**, 212. (doi:10.1186/s12862-017-1054-4)
18. Mitchell MW, Locatelli S, Clee PRS, Thomassen HA, Gonder MK. 2015 Environmental variation and rivers govern the structure of chimpanzee genetic diversity in a biodiversity hotspot. *BMC Evol. Biol.* **15**, 1. (doi:10.1186/s12862-014-0274-0)
19. Freedman AH, Thomassen HA, Buermann W, Smith TB. 2010 Genomic signals of diversification along ecological gradients in a tropical lizard. *Mol. Ecol.* **19**, 3773–3788. (doi:10.1111/j.1365-294X.2010.04684.x)
20. Smith TB, Calsbeek R, Wayne RK, Holder KH, Pires D, Bardeleben C. 2005 Testing alternative mechanisms of evolutionary divergence in an African rain forest passerine bird. *J. Evol. Biol.* **18**, 257–268. (doi:10.1111/j.1420-9101.2004.00825.x)
21. Smith TB, Thomassen HA, Freedman AH, Sehgal RN, Buermann W, Saatchi S. 2011 Patterns of divergence in the olive sunbird *Cyanomitra olivacea* (Aves, Nectariniidae) across the African rainforest–savanna ecotone. *Biol. J. Linn. Soc.* **103**, 821–835. (doi:10.1111/j.1095-8312.2011.01674.x)
22. Heuertz M, Duminil J, Dauby G, Savolainen V, Hardy OJ. 2014 Comparative phylogeography in rainforest trees from Lower Guinea, Africa. *PLoS ONE* **9**, e84307. (doi:10.1371/journal.pone.0084307)
23. Ellegren H. 2014 Genome sequencing and population genomics in non-model organisms. *Trends Ecol. Evol.* **29**, 51–63. (doi:10.1016/j.tree.2013.09.008)
24. Stapley J, Reger J, Feulner PG, Smadja C, Galindo J, Ekblom R. 2010 Adaptation genomics, the next generation. *Trends Ecol. Evol.* **25**, 705–712. (doi:10.1016/j.tree.2010.09.002)
25. Ellis N, Smith SJ, Pitcher CR. 2012 Gradient forests, calculating importance gradients on physical predictors. *Ecology* **93**, 156–168. (doi:10.1890/11-0252.1)
26. Ferrier S, Manion G, Elith J, Richardson K. 2007 Using generalized dissimilarity modelling to analyse and predict patterns of beta diversity in regional biodiversity assessment. *Divers. Distrib.* **13**, 252–264. (doi:10.1111/j.1472-4642.2007.00341.x)
27. Fitzpatrick MC, Keller SR. 2015 Ecological genomics meets community-level modelling of biodiversity, mapping the genomic landscape of current and future environmental adaptation. *Ecol. Lett.* **18**, 1–16. (doi:10.1111/ele.12376)
28. Gugger PF, Liang CT, Sork VL, Hodgskiss P, Wright JW. 2018 Applying landscape genomic tools to forest management and restoration of Hawaiian koa (*Acacia koa*) in a changing environment. *Evol. Appl.* **11**, 231–242. (doi:10.1111/eva.12534)
29. Jia KH *et al.* 2020 Landscape genomics predicts climate change-related genetic offset for the widespread *Platykladus orientalis* (Cupressaceae). *Evol. Appl.* **13**, 665–676. (doi:10.1111/eva.12891)
30. Martins K *et al.* 2018 Landscape genomics provides evidence of climate-associated genetic variation in Mexican populations of *Quercus rugosa*. *Evol. Appl.* **11**, 1842–1858. (doi:10.1111/eva.12684)
31. Nicolas V, Missouip AD, Denys C, Kerbis Peterhans J, Katuala P, Couloux A, Colyn M. 2011 The roles of rivers and Pleistocene refugia in shaping genetic diversity in *Praomys misonnei* in tropical Africa. *J. Biogeogr.* **38**, 191–207. (doi:10.1111/j.1365-2699.2010.02399.x)
32. Nicolas V *et al.* 2010 Molecular and morphometric variation in two sibling species of the genus *Praomys* (Rodentia, Muridae), implications for biogeography. *Zool. J. Linn. Soc.* **160**, 397–419. (doi:10.1111/j.1096-3642.2009.00602.x)
33. Roberts RB, Hu Y, Albertson RC, Kocher TD. 2011 Craniofacial divergence and ongoing adaptation via the hedgehog pathway. *Proc. Natl Acad. Sci. USA* **108**, 13 194–13 199. (doi:10.1073/pnas.1018456108)
34. Frichot E, Schoville SD, Bouchard G, François O. 2013 Testing for associations between loci and environmental gradients using latent factor mixed models. *Mol. Biol. Evol.* **30**, 1687–1699. (doi:10.1093/molbev/mst063)
35. Mboumba J-F *et al.* 2019 Comparative efficiency of three bait types for live trapping small rodents in central Africa. *Int. J. Biodivers. Conserv.* **11**, 85–89. (doi:10.5897/IJBC2018.1249)
36. Ali OA, O'Rourke SM, Amish SJ, Meek MH, Luikart G, Jeffres C, Miller MR. 2016 RAD capture (Rapture), flexible and efficient sequence-based genotyping. *Genetics* **202**, 389–400. (doi:10.1534/genetics.115.183665)
37. Catchen J, Hohenlohe PA, Bassham S, Agmores A, Cresko WA. 2013 Stacks, an analysis tool set for population genomics. *Mol. Ecol.* **22**, 3124–3140. (doi:10.1111/mec.12354)
38. Li H, Durbin R. 2009 Fast and accurate short read alignment with Burrows–Wheeler transform. *Bioinformatics* **25**, 1754–1760. (doi:10.1093/bioinformatics/btp324)
39. Li H *et al.* 2009 The sequence alignment/map format and SAMtools. *Bioinformatics* **25**, 2078–2079. (doi:10.1093/bioinformatics/btp352)
40. Klingenberg CP. 2011 MorphoJ, an integrated software package for geometric morphometrics. *Mol. Ecol. Resour.* **11**, 353–357. (doi:10.1111/j.1755-0998.2010.02924.x)
41. Klingenberg CP, Monteiro LR. 2005 Distances and directions in multidimensional shape spaces, implications for morphometric applications. *Syst. Biol.* **54**, 678–688. (doi:10.1080/10635150590947258)
42. Klingenberg CP, McIntyre GS. 1998 Geometric morphometrics of developmental instability, analysing patterns of fluctuating asymmetry with Procrustes methods. *Evolution* **52**, 1363–1375. (doi:10.1111/j.1558-5646.1998.tb02018.x)
43. Sesink CPR. 2017 Distributions, drivers, and risks of wildlife infectious diseases across Africa, using geospatial analyses to elucidate disease occurrence in biodiversity hotspots. Doctoral dissertation, Philadelphia, Drexel University.
44. Riahi K, Rao S, Krey V, Cho C, Chirkov V, Fischer G, Kindermann G, Nakicenovic N, Rafaj P. 2011 RCP 8.5—a scenario of comparatively high greenhouse gas emissions. *Clim. Change* **109**, 33. (doi:10.1007/s10584-011-0149-y)
45. McRae BH, Shah VB. 2009 *Circuitscape user's guide*. Santa Barbara, CA: The University of California.
46. Phillips SJ, Dudik M, Schapire RE. 2017 Maxent software for modeling species niches and distributions (Version 3.4.1). See http://biodiversityinformatics.amnh.org/open_source/maxent/.
47. R Core Team. 2018 *R: a language and environment for statistical computing*. Vienna, Austria: R Foundation for Statistical Computing. See <https://www.R-project.org/>
48. Liaw A, Wiener M. 2002 Classification and regression by randomForest. *R News* **2**, 18–22.
49. Raj A, Stephens M, Pritchard JK. 2014 fastSTRUCTURE, variational inference of population structure in large SNP data sets. *Genetics* **197**, 573–589. (doi:10.1534/genetics.114.164350)
50. Funk C *et al.* 2015 The climate hazards infrared precipitation with stations: a new environmental record for monitoring extremes. *Sci. Data* **2**, 150066. (doi:10.1038/sdata.2015.66)
51. Oates JF, Bergl RA, Linder JM (eds). 2004 *Africa's Gulf of Guinea forests, biodiversity patterns and conservation priorities*. New York, NY: Wildlife Conservation Society.
52. Charles KL *et al.* 2018 Sky, sea, and forest islands, diversification in the African leaf-folding frog *Afraxalus paradorsalis* (Anura, Hyperoliidae) of the Lower Guineo-Congolian rain forest. *J. Biogeogr.* **45**, 1781–1794. (doi:10.1111/jbi.13365)
53. Katuala PG, Hart JA, Hutterer R, Leirs H, Dudu A. 2005 Biodiversity and ecology of small mammals (rodents and shrews) of the Réserve de Faune à Okapis, Democratic Republic of the Congo. *Belg. J. Zool.* **135**, 191–196.
54. Monteiro LR, Duarte LC, dos Reis SF. 2003 Environmental correlates of geographical variation in skull and mandible shape of the punaré rat *Thrichomys apereoides* (Rodentia, Echimyidae). *J. Zool.* **261**, 47–57. (doi:10.1017/S0952836903003893)

55. Souto-Lima RB, Millien V. 2014 The influence of environmental factors on the morphology of red-backed voles *Myodes gapperi* (Rodentia, Arvicolinae) in Québec and western Labrador. *Biol. J. Linn. Soc.* **112**, 204–218. (doi:10.1111/bij.12263)
56. Martínez JJ, Millien V, Simone I, Priotto JW. 2014 Ecological preference between generalist and specialist rodents, spatial and environmental correlates of phenotypic variation. *Biol. J. Linn. Soc.* **112**, 180–203. (doi:10.1111/bij.12268)
57. Samuels JX. 2009 Cranial morphology and dietary habits of rodents. *Zool. J. Linnean Soc.* **156**, 864–888. (doi:10.1111/j.1096-3642.2009.00502.x)
58. Longman KA, Jenik J. 1992 Forest-savanna boundaries, general considerations. In *Nature and dynamics of forest-savanna boundaries* (eds P Furley, J Ratter, J Proctor), pp. 3–20. Dordrecht, The Netherlands: Springer.
59. Harper KA, Macdonald SE, Burton PJ. 2005 Edge influence on forest structure and composition in fragmented landscapes. *Cons. Biol.* **19**, 768–782. (doi:10.1111/j.1523-1739.2005.00045.x)
60. Athanason MG *et al.* 2016 Quantitative proteomic profiling reveals hepatic lipogenesis and liver X receptor activation in the PANDER transgenic model. *Mol. Cell. Endocrinol.* **436**, 41–49. (doi:10.1016/j.mce.2016.07.009)
61. Nakagawa T, Lomb DJ, Haigis MC, Guarente L. 2009 SIRT5 Deacetylates carbamoyl phosphate synthetase 1 and regulates the urea cycle. *Cell* **137**, 560–570. (doi:10.1016/j.cell.2009.02.026)
62. Tao YX *et al.* 2003 Impaired NMDA receptor-mediated postsynaptic function and blunted NMDA receptor-dependent persistent pain in mice lacking postsynaptic density-93 protein. *J. Neurosci.* **23**, 6703–6712. (doi:10.1523/JNEUROSCI.23-17-06703.2003)
63. Reinhard JR, Kriz A, Galic M, Angliker N, Rajalu M, Vogt KE, Ruegg MA. 2016 The calcium sensor Copine-6 regulates spine structural plasticity and learning and memory. *Nat. Commun.* **7**, 1–14. (doi:10.1038/ncomms11613)
64. Brooks TM *et al.* 2006 Global biodiversity conservation priorities. *Science* **313**, 58–61. (doi:10.1126/science.1127609)
65. Zimkus BM, Larson JG. 2013 Assessment of the amphibians of Batéké Plateau National Park, Gabon, including results of chytrid pathogen tests. *Salamandra* **49**, 150–170.
66. Walters G. 2012 Customary fire regimes and vegetation structure in Gabon's Batéké Plateau. *Hum. Ecol.* **40**, 943–955. (doi:10.1007/s10745-012-9536-x)
67. Morgan K *et al.* 2020 Data from: Precipitation and vegetation shape patterns of genomic and craniometric variation in the central African rodent *Praomys misonnei*. Dryad Digital Repository. (<https://doi.org/10.5061/dryad.0k6djh9x8>)